INTERNATIONAL JOURNAL FOR NUMERICAL METHODS IN FLUIDS, VOL. 14, 1473–1484 (1992)

NUMERICAL INVESTIGATION OF CONFINED WAKES BEHIND A SQUARE CYLINDER IN A CHANNEL

A. MUKHOPADHYAY, G. BISWAS AND T. SUNDARARAJAN

Department of Mechanical Engineering, Indian Institute of Technology, Kanpur (UP) 208016, India

SUMMARY

The structure of confined wakes behind a square cylinder in a channel is investigated via the numerical solution of the unsteady Navier–Stokes equations. Vortex shedding behind the cylinder induces periodicity in the flow field. Details of the phenomenon are simulated through numerical flow visualization. The unsteady periodic wake can be characterized by the Strouhal number, which varies with the Reynolds number and the blockage ratio of the channel. The periodicity of the flow is, however, damped in the downstream region of a long duct. This damping may be attributed to the influence of side walls on the flow structure.

KEY WORDS Bluff body Wake Vortex shedding Unsteady periodic flow

INTRODUCTION

The oscillation of chimney stacks and other structures in transverse flows is caused by vortex shedding. An initially smooth and steady flow across a bluff body may bring about damaging deflections of the body in cases where the natural frequency of the obstacle is close to the shedding frequency of the vortices. If we concentrate on the wake region where a Karman vortex street has been formed behind a bluff body, we shall observe that the wake zone undulates like a flag from side to side. These alternating deflections of the wake induce periodicity in the entire flow field. As a result the forces on the bluff body become periodic and culminate in vibration that can be detected from the oscillation of the bluff body. If this excitation frequency synchronizes with the natural frequency of the bluff body, the phenomenon of resonance is the obvious outcome. Hence unsteady flows about bluff bodies are of direct relevance to the design of structures, road vehicles, heat exchangers and wherever flow-induced vibration is important.

The vortex structure in the wake of a circular cylinder has been investigated both experimentally[1,2] and numerically.[3,4] Numerical and experimental investigations have shown that vortex shedding behind a circular cylinder in an unbounded medium starts at a Reynolds number of about 40 and that periodicity is induced in the flow field.[5] The study of vortex shedding behind rectangular/square cylinders has also been a subject of investigation for many researchers. A systematic study of eddies behind a rectangular cylinder has been undertaken by Okajima.[6] His experimental results show how the Strouhal number varies with the aspect ratio of the cylinder in the range of Reynolds number between 70 and 2×10^4. A recent work of Okajima[7] presented the variation in lift and drag forces, base pressure and Strouhal number of rectangular cylinders with different Reynolds numbers. His computations by the finite difference method showed good

0271–2091/92/121473–12$06.00

Received May 1991
Revised November 1991

agreement with experimental results and it was possible to detect a critical range of Reynolds number where the value of the Strouhal number changes followed by a drastic change in the flow pattern. Davis *et al.*[8] reported results of a numerical and experimental study of the flow around a rectangular cylinder in a horizontal channel. Strouhal numbers obtained from their computations are in good agreement with their measurements. Baba and Miyata[9] have studied the vortical structures of the flow around a rectangular cylinder by numerical integration of the Navier–Stokes equations and explained some features of the non-linear interaction between vortical motions of different scales. However, if a square cylinder is confined in a channel, irrespective of the shedding of vortices in the near wake, a parabolic velocity profile will evolve again at the exit of a long channel.[10] Biswas *et al.*[10] studied the structure of the laminar wake and the heat transfer in the presence of thermal buoyancy in a horizontal channel with a built-in square cylinder. On the basis of these investigations, carried out on a related topic, it can be said that the channel walls exert damping effects on the periodic flow. However, concrete inferences about the relationship between the wake zone aerodynamics and the channel walls have not been drawn so far. The purpose of the present work is to perform a numerical investigation of the influence of the Reynolds number and the channel walls on the structure of wakes behind a square cylinder in a two-dimensional duct.

STATEMENT OF THE PROBLEM

The system of interest is a horizontal channel with an obstacle in the form of a square cylinder placed inside it (Figure 1(a)). The dimensionless equations for continuity and momentum may be expressed in the following conservative form

$$D=\frac{\partial U}{\partial X}+\frac{\partial V}{\partial Y}=0, \tag{1}$$

$$\frac{\partial U}{\partial \tau}+\frac{\partial U^2}{\partial X}+\frac{\partial (UV)}{\partial Y}=-\frac{\partial P}{\partial X}+\frac{1}{Re}\left(\frac{\partial^2 U}{\partial X^2}+\frac{\partial^2 U}{\partial Y^2}\right), \tag{2}$$

$$\frac{\partial V}{\partial \tau}+\frac{\partial (UV)}{\partial X}+\frac{\partial V^2}{\partial Y}=-\frac{\partial P}{\partial Y}+\frac{1}{Re}\left(\frac{\partial^2 V}{\partial X^2}+\frac{\partial^2 V}{\partial Y^2}\right). \tag{3}$$

The boundary conditions of interest in this investigation are as follows. At the top and bottom surfaces of the channel

$$u=v=0.$$

At the entrance to the channel

$$\frac{u}{U_{av}}=1{\cdot}5\left[1-\left(\frac{y_m-y}{y_m}\right)^2\right], \quad v=0.$$

At the exit of the channel the continuity boundary condition is used by setting

$$\frac{\partial^2 u}{\partial x^2}=\frac{\partial^2 v}{\partial x^2}=0.$$

This ensures smooth transition through the outlet. No-slip boundary conditions for the velocities on the obstacle are used.

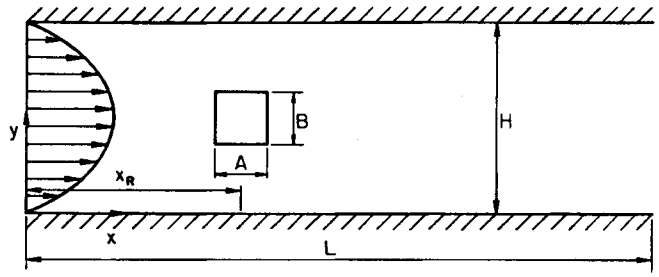

Figure 1(a). Flow in a horizontal channel with a built-in obstacle

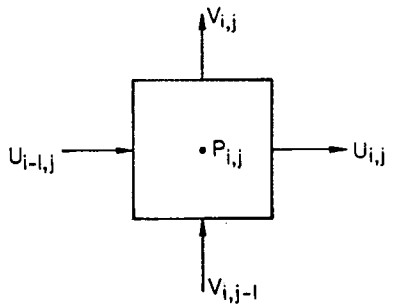

Figure 1(b). Location of velocity components and pressure on a staggered grid

METHOD OF SOLUTION

A modified version of the marker-and-cell (MAC) method[11,12] is used to obtain the numerical solution of equations (1)–(3). The computational domain is divided into Cartesian cells. Staggered grid arrangements are used in which velocity components are defined at the midpoints of the cell sides to which they are normal (Figure 1(b)). The pressure is defined at the centre of the cell.

A numerical solution is achieved by advancing through a series of small time increments $\delta\tau$. The solution is obtained in two steps. Initially an explicit calculation is performed which uses previous time velocities and pressures to determine the provisional velocities through the accelerations caused by convection, viscous stresses and pressure gradients. Fluid incompressibility is not necessarily satisfied during this explicit calculation. In order to ensure mass conservation in each cell, in a subsequent second step an iterative algorithm is employed which adjusts the velocities through changes in the pressure field. This iterative correction of explicitly advanced velocity fields through an implicit continuity equation is equivalent to the solution of a Poisson equation for pressure.[13] In the iterative pressure–velocity correction process the over-relaxation factor is chosen as 1·8. Iterations continue until the divergence-free velocity field is obtained. However, for this purpose the divergence D in each cell is towed below a preassigned small quantity (ε) after successive iterations. In our case ε is typically 10^{-4}.

In order to set the initial condition for tangential velocities, $U_{i,j}$ at each cell is taken equal to unity, i.e. $u/U_{av}=1$. Consequently, the transverse velocity component $V_{i,j}$ at each cell is taken as zero.

The conditions necessary to prevent numerical instabilities are determined from the Courant–Friedrichs–Lewy (CFL) condition and the restriction on the grid Fourier numbers.

According to the CFL conditions, the distance the fluid travels in one time increment must be less than one space increment:

$$\delta\tau < \min\left(\frac{\delta X}{|U|}, \frac{\delta Y}{|V|}\right). \tag{4}$$

When the viscous diffusion terms are more important, the condition necessary to ensure stability is dictated by the restriction on the grid Fourier numbers, which results in

$$\nu\delta\tau < \left(\frac{1}{2}\frac{\delta X^2 \delta Y^2}{\delta X^2 + \delta Y^2}\right). \tag{5}$$

The final $\delta\tau$ for each time increment is the minimum of the $\delta\tau$s obtained from (4) and (5).

A somewhat more detailed description of the solution algorithm has been discussed elsewhere.[10] The computations have been performed on a CONVEX-C220 system. The connect time and user time are 2514·3 s and 485·2 s respectively in order to perform calculations for 1000 time steps with 200×34 grids.

RESULTS AND DISCUSSION

For these computations 200×34 and 396×66 grids have been used. The computational results for 200×34 and 396×66 grids show an average difference of 3% in the peak value of $C_f Re_B$ on the channel walls. However, the computation time with 396×66 grids is nearly nine times that with 200×34 grids. It can thus be said that for most practical purposes 200×34 grids can produce grid-independent results, although for some calculations 396×66 grids were used. Uniform grids are deployed throughout the calculation domain. Computations have been carried out in a channel of length $L/H = 6{\cdot}125$. The geometrical centre of the square cylinder is located at a distance $X_R = 2{\cdot}125$ from the inlet. The channel and cylinder axes are aligned (Figure 1(a)). The aspect ratio of the cylinder is $A/B = 1$. The influence of different blockage ratios, namely $B/H = 0{\cdot}125$, 0·25, 0·3125 and 0·375, on vortex shedding was studied. The Reynolds number was used as input parameter.

The structure of the wake and its functional relationship with the Reynolds number can be observed in Figures 2 and 3. In Figure 2 a computed steady solution for $B/H = 0{\cdot}25$ and $Re_B = 37$

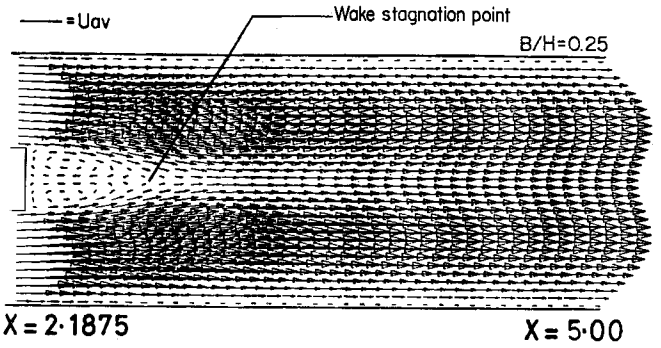

Figure 2. Attached vortices behind the cylinder in the duct: $Re_B = 37$

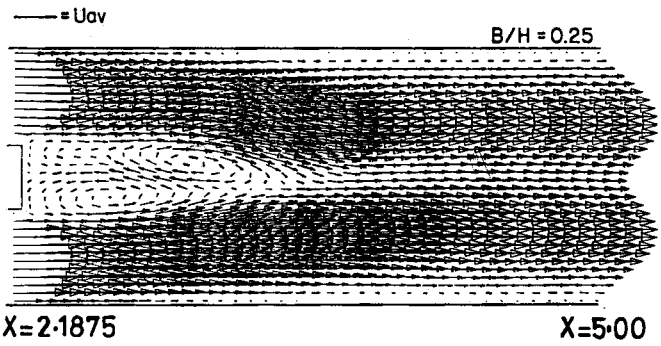

Figure 3. The wake has lost its original symmetry and is beginning to shed vortices into the stream: $Re_B=85$

is shown. The recirculating wake is extended nearly twice the obstacle width in the downstream region, but it is steady (symmetrical) and vortex shedding has not started. At $Re_B=85$ the wake loses its original symmetry and the flow becomes periodic in the near wake (Figure 3). The periodicity is suppressed downstream of the square cylinder by the channel walls and the flow at the exit of the channel tends towards steady parabolic. Davis *et al.*[8] observed periodicity in computations with the same geometrical configuration as ours at $Re_B \approx 100$. Okajima[7] found periodicity in the wake behind a rectangular cylinder in an infinite medium (blockage being negligibly small) at $Re_B=70$. From experiments with a circular cylinder in a channel, Shair *et al.*[2] report a critical Reynolds number of 130 where the wake becomes periodic. In their experiment the blockage ratio is 0·33 and the Reynolds number is defined in terms of a maximum velocity U which would exist at the same location as that of the centre of the cylinder under flow conditions identical with those of the experiment but in the absence of the cylinder. However, their transition Reynolds number describing the onset of periodicity, based on a similar definition to that of ours, would be 87 (the average velocity is two-thirds of the maximum velocity). It can be said that our Reynolds number for the onset of periodicity lies well within the range of critical Reynolds number obtained by other researchers. Finally, we may mention that Figures 2 and 3 are not merely qualitative, since the scales of the average channel velocity U_{av} are shown in the vector plots in order to make them quantitative.

Numerical calculations with higher Reynolds numbers ($Re_B>85$) confirm the shedding of vortices into the stream. With increasing Reynolds number (beyond the aforesaid transition Reynolds number) a von Karman vortex street is formed and alternate shedding of vortices into the stream becomes prominent. The vortex shedding and formation of the von Karman vortex street can be better understood from the numerical flow visualization of Figure 4. For a Reynolds number of 162 separation is observed at the leading edge followed by rolling up of vortices behind the cylinder. The flow is seen to completely detach on the lower surface of the cylinder. A favourable comparison between experimental and numerical flow visualizations has been reported by Okajima.[7] Our observation (Figure 4) of numerical flow visualization follows a similar qualitative trend to Okajima's study[7] for a Reynolds number of 150. At $Re_B=375$ the formation of the von Karman vortex street and its serpentine bends becomes prominent (Figure 5). The flow separates at the leading edge and does not reattach during a period of vortex shedding into the wake.

Figure 6 shows the time evolution of the lift coefficient for two different Reynolds numbers. In each case a periodic flow field is observed after a short transient flow. The vortex-shedding frequency can be determined from the time evolution plot of the lift coefficient distribution. The

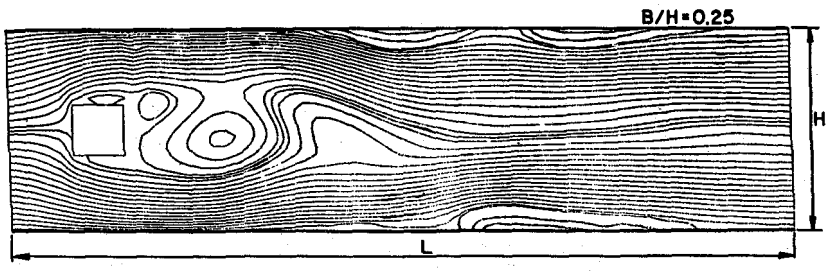

Figure 4. Streamlines crossing the cylinder in the duct: $Re_B = 162$

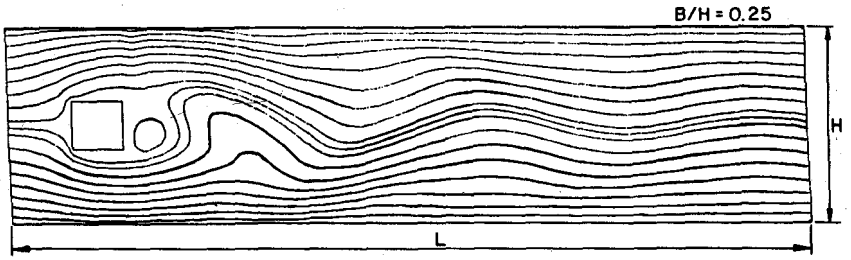

Figure 5. Streamlines crossing the cylinder in the duct: $Re_B = 375$

time period T can be calculated computationally by observing the non-dimensional time when the lift coefficient is just crossing the mean value. The difference between two such alternate time values (also shown in Figure 6) gives the time period T. Once the time period is known, the corresponding frequency ($f = 1/T$) and the Strouhal number ($S = fB/U_{av}$) can be evaluated. The periodicity is characterized by the vortex-shedding frequency or, so to speak, by the Strouhal number. The variation in the Strouhal number over a large range of Reynolds number is discussed subsequently.

The flow field in front of the cylinder seems to be nearly independent of the structure of the wake.[14] The influence of the location of the obstacle in the channel (X_R) is not of great significance with respect to the wake structure. However, for a uniform entry profile the effect of flow development will come into play. The effect of periodicity on the shear stress distribution is shown in Figure 7. It is evident that the local skin friction coefficient $C(= C_f Re_B)$ on the walls at the channel entrance is equal to 12 (the value of the fully developed laminar flow in a 2D channel) and tends to this value far downstream of the cylinder. The deviation is skin friction coefficient from 12 in front of the cylinder (at a distance of almost $2{\cdot}5B$ upstream of the cylinder) shows the upstream influence of the obstacle. It is also seen that the distribution of the skin friction C is the same on both channel walls for $Re_B = 25$ (steady flow). However, for unsteady periodic flow the situation differs considerably. For a Reynolds number of 125 we can see a remarkably changed trend in the distribution of the skin friction coefficient on the channel walls at the rear of the cylinder. Whereas the upper plate has a very high value of shear stress at $X \approx 3{\cdot}38$, on the lower plate a minimum value of shear stress is observed. One will find the opposite at a different location ($X \approx 3{\cdot}73$). This oscillating structure is damped gradually downstream of the cylinder.

The frequency f of vortex shedding was also measured by another technique. This technique borrows some ideas from the measurements of Okajima.[7] We recorded the normal component of

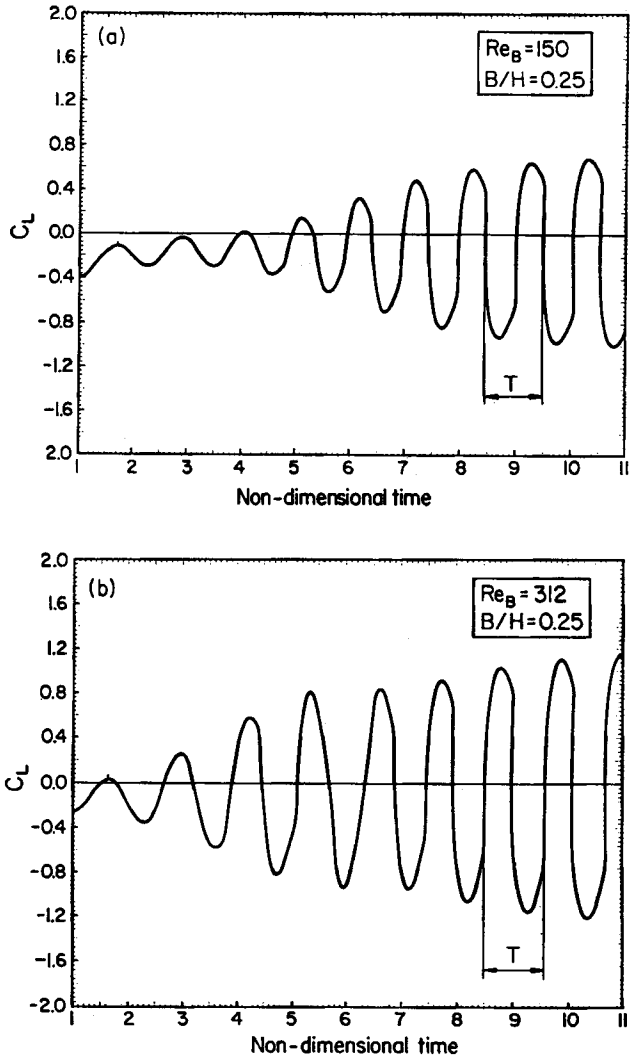

Figure 6. Time evolution of lift coefficient

velocity at a position $6B$ behind the cylinder at $y/H=0{\cdot}5$ in the wake. For steady flow the flow divides smoothly and reunites around the cylinder. As a consequence the normal component of velocity at the aforesaid location will be zero. However, for unsteady periodic flow (i.e. for high Reynolds numbers) the normal velocity component at the same location fluctuates. It is evident from Figure 8(a) that the recorded signal of the fluctuating velocity in the wake results in a sinusoidal wave. The time period T can be calculated from such signal traces, and the corresponding frequency $f(=1/T)$ and Strouhal number $S(=fB/U_{av})$ can also be found. Figure 8(b) shows the oscillation of the lift coefficient for the same Reynolds number and geometrical configuration as those of Figure 8(a). The Strouhal numbers obtained in both cases completely agree with each other ($S=0{\cdot}164$).

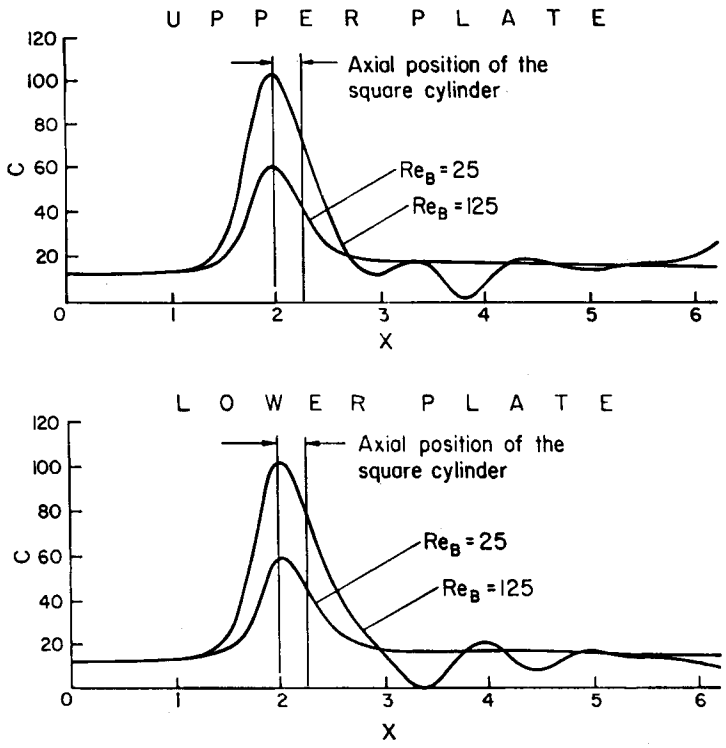

Figure 7. Variation in skin friction $C\ (=C_f Re_B)$ on the channel walls

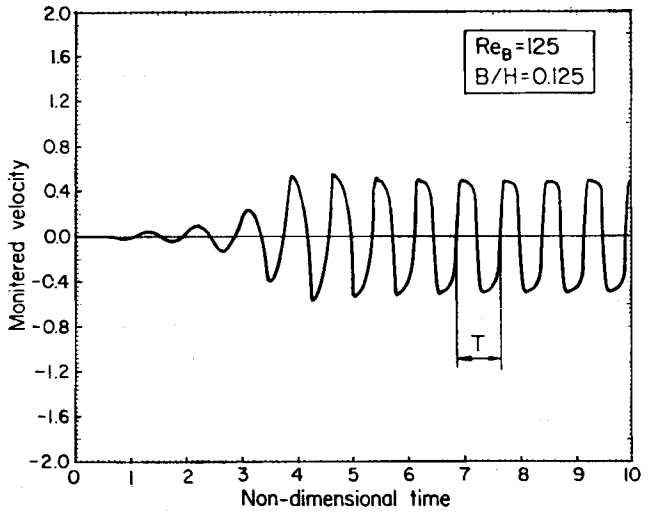

Figure 8(a). Signal traces of fluctuating velocity component in the wake

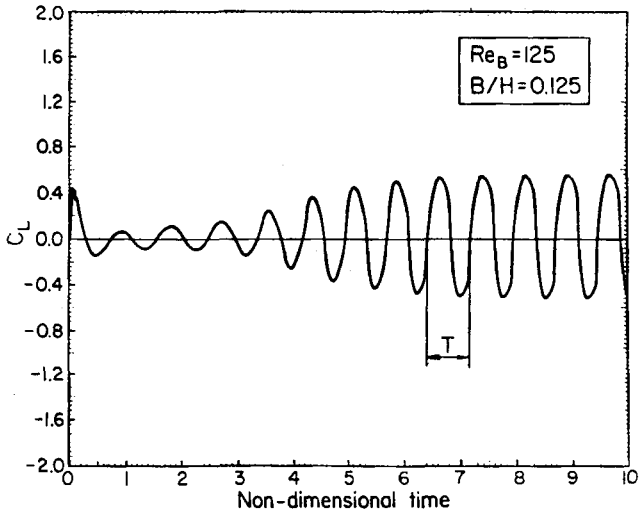

Figure 8(b). Time evolution of lift coefficient

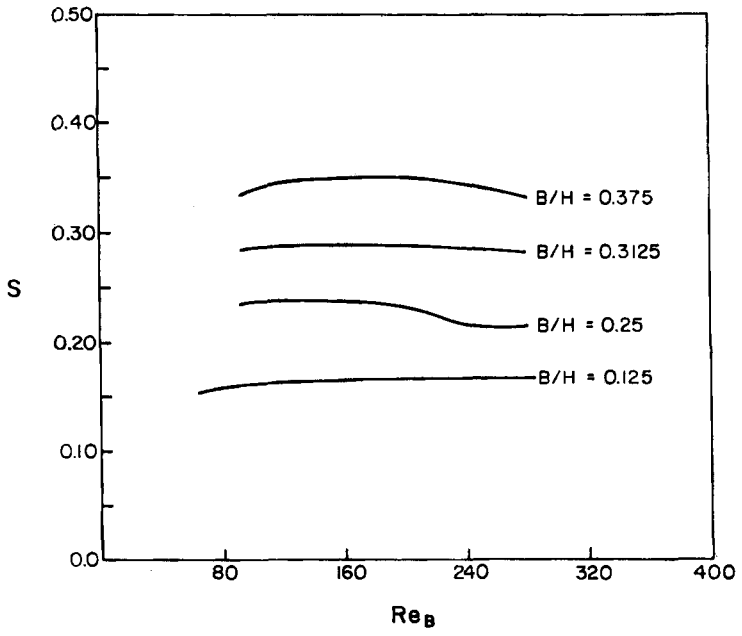

Figure 9. Effect of blockage ratio on variation in Strouhal number with Re_B

The effect of blockage ratio on the variation in Strouhal number with Re_B is shown in Figure 9. With increasing blockage ratio the value of the Strouhal number increases. In all the cases the Strouhal number undergoes a slight change with increasing Reynolds number.

At a low Reynolds number there is a steady reattachment behind the leading edge and the flow finally separates at the trailing edge, which results in symmetrical vortices. At somewhat higher

Reynolds number, after separation at the leading edge, the flow reattaches on either the upper or lower surface of the obstacle during alternate shedding of vortices into the stream. A further increase in Reynolds number causes the separated flows to detach completely from the surfaces, which eventually widens the wake and is accompanied by a relatively sharp change in Strouhal number. However, the range of Reynolds number at which the above-desired changes in the wake structure occur depends on the blockage ratio (see Figures 4, 5 and 9 and Table I).

Table I also shows the Strouhal number calculations from two methods, namely the signal traces of the fluctuating velocity components and the time evolution of the lift coefficients. The calculated values from the two methods agree with one another.

Figure 10 compares the Strouhal number distribution with the experimental results of Okajima.[7] The Strouhal number shows a continuous but slight change with Reynolds number. The present solution yields a somewhat higher Strouhal number for the entire range of Reynolds number. This discrepancy between the experimental and calculated results can be explained by noting that the experiments were done for a negligibly small blockage ratio. Although our

Table I

Observation number	$Re_B = U_{av}B/\nu$	B/H	Strouhal number $S = fB/U_{av}$	
			From time evolution of lift coefficient	From signal traces of fluctuating velocity
1	60	0·125	0·1521	0·1520
2	70	0·125	0·1551	0·1556
3	80	0·125	0·16	0·159
4	100	0·125	0·1623	0·162
5	125	0·125	0·164	0·164
6	200	0·125	0·1668	0·1669
7	300	0·125	0·167	0·167
8	400	0·125	0·1672	0·1676
9	500	0·125	0·1672	0·1676
10	600	0·125	0·1674	0·1674
11	800	0·125	0·1651	0·1654
12	87	0·25	0·236	0·237
13	112	0·25	0·238	0·238
14	150	0·25	0·2384	0·2384
15	200	0·25	0·235	0·235
16	250	0·25	0·212	0·210
17	312	0·25	0·22	0·22
18	375	0·25	0·212	0·211
19	500	0·25	0·217	0·216
20	625	0·25	0·213	0·2128
21	87	0·3125	0·2845	0·2853
22	112	0·3125	0·2875	0·2887
23	150	0·3125	0·2913	0·2897
24	200	0·3125	0·2914	0·2886
25	250	0·3125	0·2885	0·2859
26	312	0·3125	0·2842	0·2778
27	87	0·375	0·3317	0·3316
28	112	0·375	0·3452	0·3454
29	150	0·375	0·3488	0·3489
30	200	0·375	0·3506	0·3511
31	250	0·375	0·3566	0·3423
32	312	0·375	0·3337	0·3203

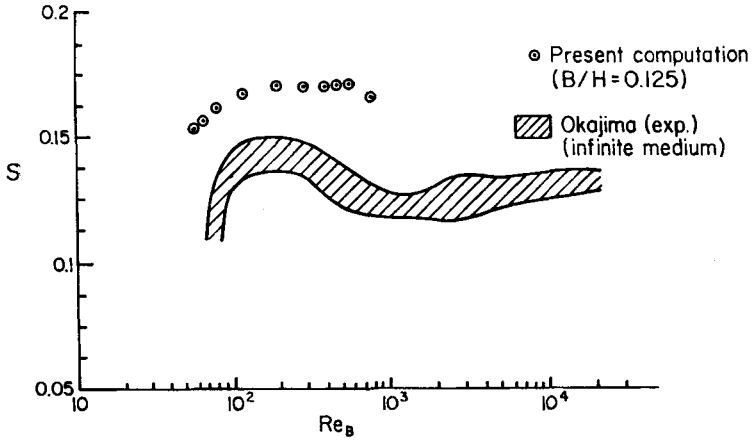

Figure 10. Variation in Strouhal number with Reynolds number for a square cylinder

predictions were done for a very small blockage ratio ($B/H = 0{\cdot}125$), one may conjecture that the influence of side walls could not be completely ignored. The finite blockage might have brought about some change in Strouhal number.

The fluctuating velocity signal was measured at various other locations in the duct. The frequency of oscillation for a particular situation (i.e. fixed Reynolds number and blockage ratio) at different spatial locations was found to be the same. Far downstream the amplitude becomes so low that the oscillation becomes insignificant. Possibly because of this, in a long duct the von Karman vortex street is gradually damped out and a steady parabolic profile reappears near the exit.

ACKNOWLEDGEMENT

The authors gratefully acknowledge the valuable suggestions of the reviewer which have helped in revising the paper.

APPENDIX: NOMENCLATURE

A	length of square cylinder
B	width of square cylinder
C	a parameter, $Re_B c_f$
c_f	skin friction coefficient, $2\mu\,(\partial u/\partial y)_w/\rho U_{av}^2$
C_L	lift coefficient, $\mathscr{L}/\frac{1}{2}\rho U_{av}^2 A$
D	divergence of velocity vectors, equation (1)
f	frequency of vortex shedding
H	width of channel
L	length of channel
$\mathscr{L}$	lift force on cylinder, $\sum \tilde{P}_1 \Delta x - \sum \tilde{P}_2 \Delta x$
n	iterations in time step
p	pressure
P	non-dimensional pressure, $p/\rho U_{av}^2$
$\tilde{P}$	pressure distribution on cylinder surface
Re_B	Reynolds number based on cylinder width, $U_{av}B/\nu$

S Strouhal number, fB/U_{av}
T time period of oscillation, $1/f$
t time
u axial component of velocity
U non-dimensional axial velocity, u/U_{av}
v normal component of velocity
V non-dimensional normal velocity, v/U_{av}
x axial dimension of co-ordinates
X x/H
y normal dimension of co-ordinates
Y y/H

Greek letters

μ dynamic viscosity of fluid
ν kinematic viscosity of fluid
ρ density of fluid
τ non-dimensional time, $t/(H/U_{av})$

Subscripts

1 bottom surface of obstacle
2 top surface of obstacle
av average
m channel midplane ($y_m = H/2$)
w channel wall

REFERENCES

1. A. Acrivos, D. D. Snowden, A. S. Grove and E. E. Petersen, 'The steady separated flow past a circular cylinder at large Reynolds number', *J. Fluid Mech.*, **21**, 737–760 (1965).
2. F. H. Shair, A. S. Grove, E. E. Petersen and A. Acrivos, 'The effect of confining walls on the stability of the steady wake behind a circular cylinder', *J. Fluid Mech.*, **17**, 546–550 (1963).
3. D. C. Thoman and A. A. Szewczyk, 'Time dependent viscous flow over a circular cylinder', *Phys. Fluids, Suppl. II*, **12**, 76–87 (1969).
4. C. C. S. Song and M. Yuan, 'Simulation of vortex shedding flow about a circular cylinder at high Reynolds numbers', *J. Fluids Eng. (ASME)*, **112**, 155–164 (1990).
5. M. Van Dyke, *An album of Fluid Motion*, Department of Mechanical Engineering, Stanford University, Stanford, CA, 1982.
6. A. Okajima, 'Strouhal numbers of rectangular cylinders', *J. Fluid Mech.*, **123**, 379–398 (1982).
7. A. Okajima, 'Numerical simulation of flow around rectangular cylinders', *J. Wind Eng. Ind. Aerodyn.*, **33**, 171–180 (1990).
8. R. W. Davis, E. F. Moore and L. P. Purtell, 'A numerical and experimental study of confined flow around rectangular cylinders', *Phys. Fluids*, **27**, 46–59 (1984).
9. N. Baba and H. Miyata, 'Numerical study of the 3D separating flow about obstacles with sharp corners', in D. L. Dwoyer, M. Y. Hussaini and R. G. Voigt (eds), *Proc. 11th Int. Conf. on Numerical Methods in Fluid Dynamics*, Springer, Berlin/Heidelberg, 1989, pp. 126–130.
10. G. Biswas, H. Laschefski, N. K. Mitra and M. Fiebig, 'Numerical investigation of mixed convection heat transfer in a horizontal channel with a built-in square cylinder', *Numer. Heat Transfer A*, **18**, 173–188 (1990).
11. F. H. Harlow and J. E. Welch, 'Numerical calculation of time-dependent viscous incompressible flow of fluid with free surface', *Phys. Fluids*, **8**, 2182–2188 (1965).
12. C. W. Hirt and J. L. Cook, 'Calculating three-dimensional flows around structures and over rough terrain', *J. Comput. Phys.*, **10**, 324–340 (1972).
13. J. A. Viecelli, 'A computing method for incompressible flows bounded by moving walls', *J. Comput. Phys.*, **8**, 119–143 (1971).
14. P. Kiehm, N. K. Mitra and M. Fiebig, 'Numerical investigation of two- and three-dimensional confined wakes behind a circular cylinder in a channel', *AIAA Paper 86-0035*, 1986.